IRAQI Academic Scientific Journals

Al-Rafidain Engineering Journal (AREJ) Vol.28, No.1, March 2023, pp. 145-164

A Review of Miniaturized Advanced IC Rectenna for Energy Harvesting Applications

Shamil H. Hussein
shamil_alnajjar84@uomosul.edu.iq

Khalid K. Mohammed
khalid.khaleel@uomosul.edu.iq

Electrical Engineering Department, Collage of Engineering, University of Mosul, Mosul, Iraq

Received: 2022-08-31 Received in revised form: 2022-09-27 Accepted: 2022-10-07

ABSTRACT

This article presents a review of different types of miniaturized rectenna integrated circuits IC used for energy harvesting applications such as medical applications. The rectenna design consists of two basic components: an embedded antenna that collects radio-frequency RF energy from the surrounding environment, and the rectifier circuit that converts AC-RF energy values into DC voltage for usage in low-power electronics devices such as implantable medical devices (IMDs). Microwave Schottky diodes HSMS-285x and SMS-763x series are used as a voltage doubler rectifier with an implanted antenna to improve conversion efficiency and the output voltage at a given input power and appropriate load. There are many challenges in the implantable rectenna IC design such as biocompatibility, miniaturization, patient safety, compact size, resonant frequency, bandwidth, radiation efficiency, and insensitivity to detuning. This review article summarizes the overall rectenna research carried out for new different design strategies in implant medical applications that operated at industrial scientific, and medical (ISM) bands such as 2.45GHz and 5.8GHz.

Keywords:

Rectenna Integrated Circuits, Microwave Schottky diodes, Energy harvesting, and implantable Antennas

1. INTRODUCTION

In recent years, the growing global demand for clean renewable energy is a vital issue with major economic and social implications for our planet's future [1]. Therefore, the energy harvesting has become very important by collecting energy from surrounding environments. Energy harvesting sources may be captured from the ambient environment or external [2]. Ambient Energy is the process by which energy is derived from external sources [3], such as solar energy [4], wind energy [5], thermal energy [6], vibration-sourced piezoelectric [7], and electromagnetic ambient signals which involve radio-frequency RF energy [8], near electromagnetic field [9], and far-field electromagnetic signals [10]. The constant source of energy harvesting is the sun which captures rays by using solar cells. The cells represent the green energy that protects the environment from pollution. But the limitations of solar cells are little efficiency. Therefore, there are other solar inverter alternatives, such as radio frequency (RF) energy harvesting [11].

The main focus of this review paper is on using rectenna circuits for energy harvesting applications which are used to capture environmental RF signals and convert them to DC voltage to drive low-power electronic devices. The basic structure of the rectenna consists of an implant antenna, rectifier circuit, harmonic regression filter ,and load resistance as shown in Fig. 1. These systems combine various research fields that have a bright future for generating power to run low-power biomedical electronic devices such as IMDs [12], wireless sensor networks WSNs [13], wireless energy harvesting [14], and wireless power transmission WPT [15].

The IMD devices have recently attracted the attention of scientists due to people are increasingly using these devices such as pacemakers [16], pill cameras [17], artificial arms, and measure human blood pressure and sugar in real time [18] as a result of recent advancements in the health-care system and especially after COVID 19 occurrence. Wireless charging is required for IMD devices that are implanted in the human body. This means that the IMD should be powered without touching it to avoid electromagnetic radiation coupling with human tissue. Because human tissue is very sensitive and absorbs the majority of the power going through it, it is one of the major issues in the field of biomedical electromagnetic engineering.

The first theoretical knowledge about WPT dates back to 1864 by Maxwell [19]. Subsequently, Nikola Tesla, at the end of the 19th century, carried out numerous experiments on the transmission of electricity without wires [20]. However, these experiments were unsuccessful because they used a frequency of 150 kHz. There are two techniques of WPT used in IMDs : electromagnetic (EM) and non-EM energy. The distance between the transmitter and IMD devices of the WPT systems can be divided into three: First of them, the non-radiative less than 100mm such as capacitive [21], inductive [22], and magnetic resonance coupling [23]. While the radiative mid-field WPT is characterized by the distance of 100 to 500mm [24]. The far-field system of WPT such as optical coupling with more than 500mm distance transmission [25]. The non-EM energy technique is acoustic- based WPT [26]. In this review paper by using tables, we will present many challenges and characteristics of the rectenna design such as the compact size of the IMDs receiver, the distance of the WPT, Power conversion efficiency (PCE), power gain, and tissue safety in the body.

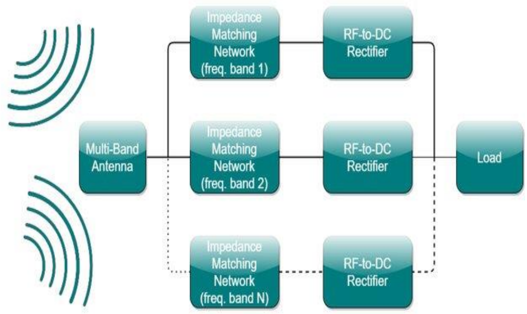

Fig.1. Block diagram of the typical multi-band rectenna IC system [27].

The implanted antenna operates as a receiver to collect ambient RF signals, as shown in Fig. 1. There are many different types of embedded antenna designs with diverse shapes and features, including micro-strip patch, planar dipole, Folded dipole, spiral, and circular polarized antennas. Also, there are four types of rectifier configurations: series/shunt, half-wave HWR, full-wave bridge FWBR, and voltage doubler VDR. The voltage multiplier is the best choice because it can have obtained double the amplitude of the received signal. The rectenna's load resistance is adjusted to achieve high rectifying efficiency and output DC voltage. As mentioned above the main challenges in rectenna design for IMD are compact size and high efficiency. To improve that, there has been much research aimed at these. Firstly, Dalia H. Sadek et al. in 2021 [28] proposed a new configuration of the compact rectenna circuit for dedicated far-field RF wireless power-harvesting applications.

Diamond slot ground was used to design and fabricate a triple band L-Arms microstrip patch antenna as well as two rectifier circuits. The resonance frequency bands are 10, 13, 17, and 26GHz with 10-dB impedance bandwidth of 0.67, 0.8, 2.45, and 4.3GHz, respectively. In [29][30][31], arrays of antennas are employed to enhance the antenna's gain and hence its efficiency. Also, a buck-boost converter was presented by Yadav and Ray in 2021 to improve efficiency and output voltage [32]. Several techniques are used to improve the compact size and PCE such as the T-shape, U-shape slots, and circular shape slots that proposed by Chindhi in 2022 [33] and Xu in [34]. VDR rectifiers with the ground coplanar waveguide are used in [35] to improve PCE. Mishu and Song use CMOS bridge rectifiers to increase WPT in energy harvesting applications [36].

In this paper, we present a systematic review of rectenna based on the system design, optimization methodology, performance, and implementation of the WPT technology for IMD devices. The paper is organized as follows. The geometrical description of the implant antenna design is explained in section II, together with all relevant parameters. The presented antenna covers bands such as ISM, and Medical Implant Communication System (MICS). In section-II, deals with the wave interaction problems between the external transmitter and implant antenna. In section-III, a realistic rectifying circuit simulation will be studied. In section-IV, analysis and design of the miniaturized implant rectenna IC for IMD as well as a comparison of other studies. Finally, the conclusion is discussed in section V followed by references. The target of this paper is to describe a complete embedded rectenna's working scenario.

2. ANALYSIS AND DESIGN OF THE IMPLANTABLE ANTENNA

There are several challenges in the growth of IMDs devices, which have been studied in deepness in current years with RF energy harvesting. As a result, this review focuses on antenna design and definition while the human body is present, as well as introducing novel designs that handle several of the existing challenges, such as integration, efficiency, miniaturization, and frequency detuning. Also, in order to improve the performance of the implant antenna inside human tissue, it should be taken into consideration the interaction between embedded antennas and biological tissues which represent electrical permittivity (ε) and electrical conductivity (σ) [37]. The requirements and challenges related to the design of implantable micro-strip or dipole antennas in the presence of a human body are as follows.

2.1. Frequency of Operation

There are many techniques of the WPT systems used in IMDs devices. First of them, inductive coupling is operated at a frequency of 15MHz, and then RF bands such as MICS, and ISM bands. [38]. In order to achieve small antenna sizes, can be used at high frequency with maintained to low power loss. The implant antennas field regions are the most essential factor that is changed by the operating frequency. The most important challenge of the implant antenna design is the efficiency is reduced when an antenna is implanted in bio-tissues that operate with several frequency bands and transition regions. Table 1 shows the regions of reactive, radiation near-field, transition zone, and far-field of the antenna which worked in medical bands such as 403 MHz, 866 MHz, and 2.45 GHz [39]. Finally, we conclude that the operating frequency of the antenna is inversely proportional with area size and distance between the transmitter antenna (Tx) and the implant receive antenna (Rx).

Table 1. Field regions for implant antenna based on the ISM medical bands [39]

Radiative Regions	Distance between Tx and Rx in [mm]	403 [MHz]	866 [MHz]	2.45 [GHz]
Reactive near-field	0.159λ	17.3	8.5	3.2
Radiative near-field	λ	108.9	52.7	19.9
Transition zone	2λ	217.8	107.4	39.7

2.2. Patient Safety and Phantom Tissues

The specific absorption rate (SAR) is the rate of energy deposited per unit mass of tissues. Two standard restrictions of SAR averaged are 1g and 10g tissue in the shape of a cube for the IEEE C95.1-1999 USA and IEEE C95.1-2005 Europe standard respectively. Thus, the patient safety of the human tissues is 1.6W/kg and 2W/kg [40].

Depending on the application, the phantom dimensions are frequently chosen. Another important factor for antenna performance is implant placement. The amount of lossy tissue that must be penetrated by the EM radiation depends on the implant depth [41]. As demonstrated in table 2, the dielectric characteristics of living tissues (skin, fat, and muscle) alter with frequency.

Table 2. Dielectric characteristics of human tissue at various frequencies [42]

	ε_r			σ [S/m]		
Freq. bands [MHz]	403	868	2450	403	868	2450
Skin	46.72	41.58	38.01	0.689	0.856	1.464
Fat	5.58	5.47	5.28	0.041	0.05	0.105
Muscle	57.10	55.11	52.73	0.797	0.932	1.739
Bone	13.14	12.49	11.38	0.092	0.14	0.394

In this paper, a literature review of the several challenges of the wireless implant rectenna design for biomedical applications is shown in tables later. Biocompatibility is the most important challenge which represents the antenna system environment contacting multiple layers of the human body depicted in Fig. 2 [43]. As it is shown in Fig. 2, the compact antenna may be implanted inside layers of the human tissues such as skin, muscle, fat, and bone. Therefore, the interaction between the implant antenna and bio-tissues should be taken into consideration.

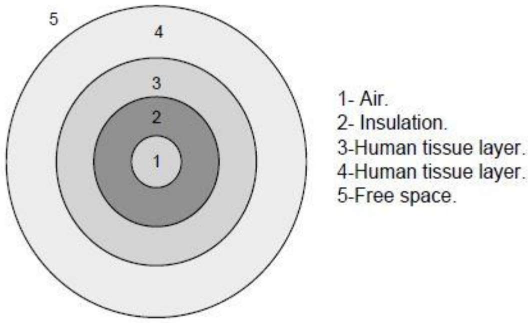

Fig. 2. Body sample: muscle, skin, and fat [43]

2.3. Antenna Characterization

In the design process and fabrication of the implantable antennas in the human body, one of the main challenges is experimental validation before it is integrated with the entire rectifier device. The far-field characterizations are reflection coefficient, gain, efficiency, and radiation pattern. The main disturbance which alters antenna performance significantly is the feeding by unbalanced coaxial cable. To prevent cable-related disruptions, a variety of techniques have been devised, including baluns, chokes, discrete ports, and ferrites [44].

2.4. Radiation Pattern and Efficiency

The radiation pattern and efficiency of the antennas are highly influenced by the framing environment, especially those in the near-field region. The radiation efficiency can be defined by the ratio of the radiated power from the antenna to the delivered value. When the directionality of the radiation pattern tends to out from the body direction, the SAR value of biological tissue and radiation efficiency for the in-body antenna is reduced. A lossless substrate has been utilized instead of a lossy medium to improve the efficiency of in-body antennas [45].

2.5. Miniaturization

Recent progress in electronic IMD technology has resulted in implantable medical device designs that are extremely small [46]. As a result, when designing the implantable antenna, miniaturization becomes one of the most significant challenges. Miniaturization is the process of reducing the size of an antenna while maintaining a suitable level of gain and PCE [47].

There are many strategies of the miniaturization techniques presented in the literature review for the implant antennas design are shown in tables 3 and 4. The most common structures for IMD antennas are micro-strip radiators, such as Planar-Inverted-F-Antenna (PIFA) due to small volumes [48], multilayer PIFA structures [49], monopoles, dipoles, and loop antennas. Several structures of the implantable antennas design can be used to get miniaturization process such as serpentines [50], and spiral structure [51] developed by Le Trong in 2021 [52] by using an open-ended slot at the ground for human head-implantable wireless communications utilizing a triple band antenna.

The meander structure is reported in [53] and developed by Nikta in 2021 [54], fractal geometries [55], Flower-shape radiating patch [56], Circular Maze shaped [57], and several geometries shaped radiator are suggested in [58] [59] [60] for energy harvesting applications. The materials with a high ε of substrate, loading, and resonance frequency are techniques used in implant antennas to achieve miniaturization.

2.6. Biocompatible

The biocompatibility of the compact implant antenna in the human body without interaction with tissues is the most critical requirement. It's used to keep patients safe and keep implants from rejecting. There are two methods for accomplishing this: separating the metallic radiator from human tissue by selecting the best substrate/superstrate materials, and biocompatible encapsulation by insertion of a thin layer. The biocompatible techniques are presented in the literature review as shown in table 5. The Teflon, ceramic alumina, zirconia, and silastic MDX-4210 are materials that have been reported in [61]. It's worth noting, however, that ceramic substrates are difficult to drill, and zirconia is a better candidate material for biocompatible insulation due to its electrical characteristics [62].

The thickness of the substrate and patch layer, which provides a biocompatible insulation layer [63]. In the literature, completely different miniaturized and biocompatible techniques have been used to reduce the size of the antenna and to ensure patient safety as shown in tables below.

Yeap, Kimho, et al. in 2019 [64], proposed a dual band CPWs fed implant monopole patch-antenna fabricated on a RO3210 substrate as shown in Fig. 3 and operated at MICS and ISM band. The antennas were implanted in the minced-pork model and the human skin tissue phantom. The measurement results show that the bandwidth of 120MHz and 40MHz for dual bands respectively is shown in Fig. 4. The size of the antenna is [22×16×1.27] mm^3 and SAR values of 0.352 and 0.054μW/kg for 1g, and 10g standard respectively. The measured return loss is -17dB and -15dB for the medical bands 402MHz and 2.45GHz respectively. The work in [64] is developed by Usluer in 2020 [65]. They proposed a new structure called complementary split-ring (CSR) is shown in Fig. 5. The proposed antenna is used for biotelemetry applications. The total size of the compact design was reduced to half the size obtained in [64] by using a CSR structure with a shorting-pin. Also, a hook-shaped slot- loaded ground plane is utilized for wideband operation. The proposed ICSRA was fabricated and measured in two different gels mimicking the real human skin tissue. The measured bandwidths obtained are (95 and 297) MHz for MICS 460MHz and ISM 2.34GHz respectively as shown in Fig. 6.

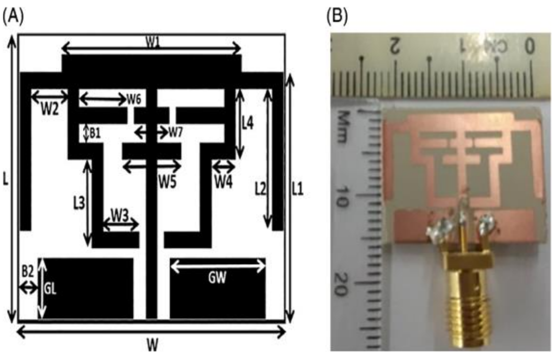

Fig. 3. Proposed implantable-antenna [64]: (A) Schematic diagram with L=16, L_1=14, L_2=8, L_3=W_5=5mm, L_4=W_6=4mm, W=22mm, W_1=15mm, W_2=W_3=W_7=3mm, W_4=2mm. (B) Photograph of the fabricated suggest antenna.

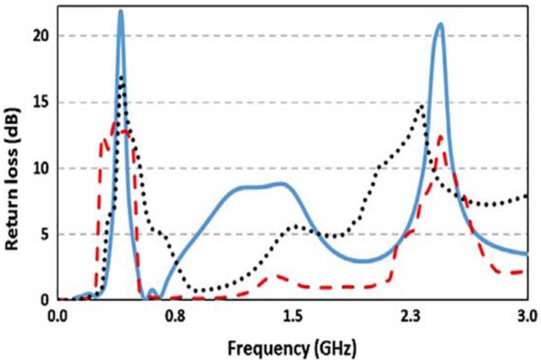

Fig. 4. Simulation and measurement return loss of the antenna. simulation (solid line), measurements (dashed line), and minced pork (dotted) [64].

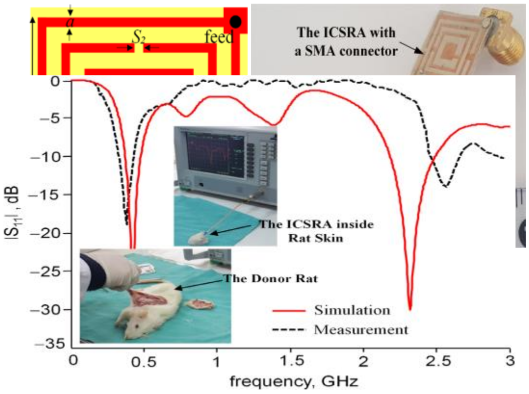

Fig. 5. Geometry of the suggested antenna and its design specifications [65].

Fig. 6. The reflection coefficient of the proposed antenna in [65].

In 2021, Wang, et al. [66] proposed a miniaturized implantable antenna with bandwidth improvement for cardiac pacemaker applications. Split resonant rings are presented to achieve ultra-wideband characteristics which can cover from 272MHz to 1504MHz. The proposed implantable antenna shown in Fig. 7 was fabricated on the substrate of RO6010. The Miniaturization technique was applied to design a compact antenna with a size [12 ×12 ×0.635] mm^3. From simulation results, the peak gain is -32dBi and -34dBi, for 403MHz and 920MHz respectively.

Seydi and Bayati proposed a new structure of the implant antenna design called rectangular meandering-micro-strip patch antenna (RM-MPA) in 2021 [67] as shown in Fig. 8. The proposed antenna operates at 2.45GHz using shorting pin technique. The Rogers 3210 has been used for substrate and superstrate with thickness of 1.27mm. The proposed antenna is simulated in free space and skin phantom with 90% of efficiency and 25MHz of bandwidth. Finally, the antenna is tested in minced meat and tissue liquid with 0.4 W/kg of SAR value.

Fig. 7. Proposed implantable antenna in 2020 [66]: (a) Top view and (b) bottom view. Dimensions in mm. l=12, a=11.5, b=10, g=0.5, w=0.5, and s=0.25.

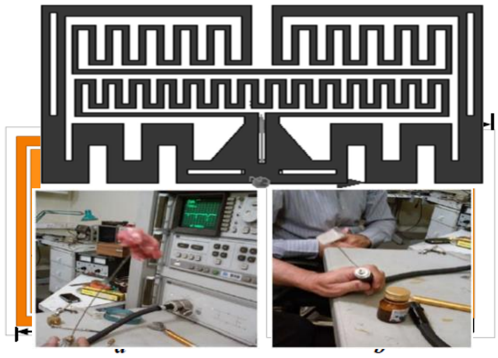

Fig. 8. Rectangular meandering- microstrip patch antenna proposed in 2021 [67].

In 2021 [68], the same authors in ref. [69], proposed a new structure of the implant antenna design for medical applications that operate at single band (402-405) MHz. The overall dimensions are [$\pi \times (5)^2 \times 0.762$] mm^3. The antenna was simulated in muscle tissue phantom by using CST software. From the simulation results obtained the reflection coefficient, peak gain, and bandwidth are -15dB, -35.3dBi, and 40.5MHz respectively.

Several structures of the implant antenna design were published as shown in tables 3, 4, and 5.

Table 3. Implantable antennas performance comparison of literature review with respect miniaturization techniques.

Ref. Year	Proposed Antenna Structures	Resonant frequency [GHz]	Miniaturization Tech.		
			Short Pin	Stack Patch	Dielectric Materials
[48] 2021	Implantable circular-shaped meandered PIFA structure.	ISM 2.43	Yes	----	Rogers 3210, and FR-4. Thickness=0.7
[49] 2021	Multilayer PIFA meander miniaturized implantable for CGM.	MICS 0.402-0.405	Yes	Yes	Rogers Duroid 610LM, and FR-4.
[50] 2018	Miniaturized DGS serpentine patch.	ISM 2.4-2.48	----	Yes	Rogers RT/ Duroid5880
[51] 2020	Microstrip patch with spiral split rings.	0.915 ISM 0.433	----	----	Polyethylene with thickness of ε_r=2.26.
[52] 2021	Triple-band implant antenna with spiral connected. to a circular ground with an open-ended slot.	MICS 0.402 WMTS 1.4 ISM 2.45	Yes	Yes	Taconic RF-10, with thickness (h) of ε_r=10.
[53] 2018	Compact Meander Line Telemetry.	MICS 0.401-0.406	Yes	Yes	FR-4 with h of ε_r = 4.7
[54] 2021	Meandered triple-band PIFA structure	MICS 0.402 MICS 0.902 ISM 2.4	Yes	Yes	Rogers 3210 with ε_r=10.2, and h=0.635.
[55] 2020	Dual-band fractal implantable antenna	MICS 0.402 ISM 2.45	Yes	Yes	Rogers 3210, with h=0.635
[56] 2018	Flower-shape dual radiating patch.	MICS 0.928 ISM 2.45	Yes	Yes	Rogers ULTRALAM
[57] 2021	Miniaturized circular maze shaped implantable antenna.	ISM 2.42–2.48	Yes	Yes	Polyamide, with ε_r=4.3, and h=0.05
[58] 2019	Novel meander integrated E-shaped.	ISM 2.2-2.5	---	Yes	FR4 epoxy, with h=1.6mm
[59] 2020	Compact microstrip patch with hexagonal shaped and notch in the ground plane.	ISM 2.45	---	Yes	FR4 epoxy, with h=1.6mm and ε_r=4.3
[60] 2020	A pentagon-shaped microstrip patch with slotted ground plane.	ISM 2.45	---	Yes	FR-4, with h=1.6mm and ε_r=4.4
[62] 2021	Rectangular micro-strip antenna patch loaded with F shaped.	ISM 2.4–2.48	---	---	Teflon substrate, ε_r=2.1
[64] 2019	Dual-band CPW-fed implantable monopole patch	MICS 0.403 ISM 2.45	---	---	Rogers 3210, with h=1.27
[65] 2020	Dual-band implant complementary split-ring (CSR).	MICS 0.403 ISM 2.45	Yes	Yes	Rogers 3010, with h=1.27
[66] 2020	Miniaturized implantable with split resonant rings	MICS 0.403 ISM 0.920	---	Yes	Rogers 6010, with ε_r=10.2 and h=0.635

[67] 2022	RM-MP Rectangular Meandering patch	ISM 2.45	Yes	Yes	Rogers 3210, with h=0.635.
[68] 2021	Gosper fractal multilayer PIFA	MICS 0.402–0.405	Yes	Yes	Rogers 3010, with h=0.762
[69] 2019	Multilayer PIFA Archimedean spiral	MICS 0.403	Yes	Yes	RT/Duroid 6010LM, with ε_r=10.2
		ISM 0.435			
[70] 2020	Circular dual-band implantable antenna	MICS 0.400	---	Yes	Rogers 6010, with h=1.27
		ISM 2.45			
[71] 2020	Dual-band implant PIFA antenna	ISM 2.45	Yes	---	FR-4, with h=1.52mm
		ISM 5.2			
[72] 2018	Microstrip patch with a short pin	ISM 2.4	Yes	----	Rogers 6010, with ε_r=10.2 and h=0.635.
[73] 2019	Circular shaped fractal-patch with DGS	2.45	----	Yes	FR-4, with h=1.6mm, and ε_r=4.4
		4.22			

Table 4. Implantable antennas performance comparison of literature review with respect antenna characteristics.

Ref. Year	Proposed Antenna Structures	Return loss [dB]	Gain On-body [dBi]	B.W [MHz]	Dimension [mm]
[48] 2021	Implantable circular-shaped meandered PIFA structure.	-37	-9.4923	61.24	$\pi \times (7.5)^2 \times 1.58$
[49] 2021	Multilayer PIFA meander miniaturized implantable for CGM.	-23	-21	20	12 × 7 × 3.94
[50] 2018	Miniaturized DGS serpentine patch.	−44.3	0.991 dB	762	44.5 × 6 × 0.78
[51] 2020	Microstrip patch with spiral split rings.	-27	-38.8	68.3	14 × 14 × 3
			-38.1		
[52] 2021	Compact triple-band implant antenna with spiral connected. to a circular ground with an open-ended slot.	-18	-23	93	$\pi \times (11.2)^2 \times 0.5$
		-20	-20.5	202	
		-15	-19	444	
[53] 2018	Compact Meander Line Telemetry.	-21	---	133	30.5 × 21.02 × 1
[54] 2021	Meandered triple-band PIFA structure	-35	−43.6	90	11 × 20.5 ×1.8
		-6	−25.8	---	
		-15	−20.1	190	
[55] 2020	Dual-band fractal implantable antenna	-30	−28.1	22.8	9.5 × 9.5 × 0.635
			−31.3	13.1	
[56] 2018	Flower-shape dual radiating patch.	-42	-28.44	184.1	7 × 7.2 × 0.2
			-25.65	219.7	
[57] 2021	Miniaturized circular maze shaped implantable antenna.	-36	-23	286	7 × 7 × 0.1
[58] 2019	Novel meander integrated E-shaped.	-36	3.78	370	60 × 60 × 4.6

[59] 2020	Compact microstrip patch with hexagonal shaped and notch in the ground plane.	-25	6.14	230	100 × 100 × 1.6
[60] 2020	A pentagon-shaped microstrip patch with slotted ground plane.	-35	8.02	240	100 × 100 × 1.6
[62] 2021	Rectangular micro-strip patch loaded with F shaped slot.	-30	12	300	13 × 16 × 1.035
[64] 2019	Dual-band CPW-fed implantable monopole patch	-17	-18.5	120	22 × 16 × 1.27
		-15	-19.5	40	
[65] 2020	Dual-band implant (CSR).	-19	-46	95	14 × 14 × 1.27
		-16	-19	297	
[66] 2020	Miniaturized implantable with split resonant rings	-25	-32	272	12 × 12 × 0.635
		-32	-34	1504	
		---	-35.1	---	
[67] 2022	RM-MP Rectangular Meandering patch	-6	-17	25	9.4 × 14 × 1.27
[68] 2021	Gosper fractal multilayer PIFA	-15	-35.3	40.5	$\pi \times (5)^2 \times 0.762$
[69] 2019	Multilayer PIFA Archimedean spiral	-42	-38	35	$\pi \times (5)^2 \times 0.762$
		-25	-40.1	50	
[70] 2021	Circular dual-band implantable antenna	-24	–33.1	153	$\pi \times (10)^2 \times 2.54$
		-18	–14.55	422	
[71] 2020	Dual-band implant PIFA antenna	-20	3.77	136.3	10 × 9.5 × 1.52
		-22	2.53	73	
[72] 2018	Microstrip patch with a short pin	-15.2	-20.8	350	11 × 11 × 0.635
[73] 2019	Circular shaped fractal-patch with DGS	-37	-20.8	2570	40 × 40 × 1.6
		---	-35.1	---	

Table 5. Implantable antennas performance comparison of literature review with respect biocompatible techniques.

Ref. Year	**Antenna Volume [mm^3]**	**SAR [W/kg] at 1W of I/P power**		**Implant Tissue**	**Aims and Applications**
		1g	**10g**		
[48] 2021	279	142.5	---	Uterus	Compact implant antenna design and high bandwidth by DGS for the Investigation of Uterus Fibroids.
[49] 2021	330.9	Avg. value 1.1441	---	Blood Glucose	Communication between base station and implantable device And Glucose sensing
[50] 2018	178.3	---	---	Human's stomach	Communication between base station and implantable antenna for Ingestible Endoscopic Applications
[51] 2020	588	161.86	---	Human's Bone	Monitoring of implants in Tibia
		154.4			
[52] 2021	197.04	241	---	Human tissues / head	Novel compact, triple-band head implanted antenna for head implants and brain machine interface biotelemetry systems.
		269			
		290			

[53] 2018	641.11	---	---	Human tissues	Pacemaker application in Medical Implant Communication Services
[54] 2021	405.9	99.5	12.6	Human tissues / head	Brain-implantable biotelemetry systems. wireless data communication, far-field WPT, and switching control between sleep/wake-up mode.
		207.8	35.8		
		272	33.4		
[55] 2020	56.45	47.9	45.5	Muscle tissue	Bio-monitoring and biomedical telemetry between external and embedded patch antenna.
[56] 2018	10.08	471	52.53	Head / Skin Phantom	Wireless communication link between base station and implantable antenna for Gastro applications and skin implantations.
		313	40.44		
[57] 2021	4.9	362	38.9	Skin	Health safety regulations and allows acceptable wireless communication ranges.
[58] 2019	16560	---	---	---	WPT and Feed electronic components and battery free sensor networks.
[59] 2020	16000	---	---	---	WPT for medical devices and RF energy harvesting applications such as Wi-Fi.
[60] 2020	16000	---	---	---	WPT for medical devices and RF energy harvesting applications such as Wi-Fi.
[62] 2021	215.3	---	---	Muscle	Medical and wireless biotelemetry applications at ISM Band.
[64] 2019	447	0.352µ	---	Human skin	Medical Telemetry.
		0.054µ			
[65] 2020	249	338	---	Skin	Medical Telemetry.
		482			
[66] 2020	91.44	921	---	Human body	Cardiac pacemaker application
		881.7			
[67] 2021	167	0.4	---	Skin phantom	Biomedical applications
[68] 2021	59.8	---	---	Human muscle tissue	Biomedical implantable devices.
[69] 2019	≤60	---	---	Human muscle tissue	Biomedical implantable devices.
[70] 2021	797.96	241.5	---	Tissue liquid	Biomedical Applications.
[71] 2020	144.4	---	---	Human body	Smart Wireless Body Sensors Networks.
[72] 2018	76.35	---	---	Cubic skin	Biomedical applications.
[73] 2019	2560	---	---	Skin, Fat, Bone	Biomedical applications are required for patient's health monitoring.

3. DESCRIPTION OF THE RECTIFIER CIRCUITS DESIGN

The rectifying circuit helps in the conversion of RF signals received by antennas into an electrical DC current for IMD device battery charging. The rectifier circuit's diode is critical, therefore choosing the correct diode is imperative [74]. The overall rectenna's performance is influenced by the rectifier's performance. In [75], a VDR configuration was used to investigate the harmonic rectifier circuit.

It's difficult to design a rectifier with higher rectification efficiency when the input power is low [76]. The RF to DC conversion efficiency is the main performance metric in the rectifier analysis [77]. Schottky diodes are used to construct rectifier circuits at RF ranges because they have a low-threshold-voltage (V_{th}) or low turn on-voltage, low-series resistance (R_s), low-junction capacitance (C_{jo}), and large breakdown-voltage (V_{br}) [78]. Different schottky-diode family for rectenna's applications has been investigated in the literature, as indicated in Table 6. The rectenna's output is limited to half of the breakdown voltage. As a result, a diode with a high Vbr has a higher output voltage [79]. The SMS-7630 and HSMS-28xx diode family is found to be suitable for low and high RF input power [80].

Table 6. Schottky diode characteristic parameters [78].

Ref.	Diode Model	V_{th} [V]	R_s [Ω]	C_{jo} [pF]	V_{br} [V]	I_s [μA]
[81]	SMS 7630	0.09	20	0.14	2.0	5.0
[82]	HSMS 2852	0.15	25.0	---	3.8	3.0
[83]	HSMS 2860	0.25	6.0	---	7.0	0.05
[84]	HSMS 2850	0.15	25.0	0.18	3.8	3
[85]	HSMS 286B	0.69	6.0	0.18	7.0	0.05
[86] [87]	HSMS 2820	0.15	6.0	7.0	15.0	0.022

Much research has been published on the rectifier circuits design which is used in the rectenna systems for medical applications. DeLong proposed a 2.4GHz rectifying patch antenna system for implant medical applications in 2018 [88], which used a radiating near-field recharging approach. As a rectifying circuit integrated with an implanted antenna, the voltage quadruple circuit is used. Schottky diode is used for rectification as shown in Fig. 9(a). Fig. 9(b) shows a circuit that produced RF-DC rectification with PCE of 40% at input power of 0 dBm.

The work in Ref. [88] was developed by Daasari, et al. in 2021 [89] through increased PCE and output voltage. They proposed a VDR circuit to be applied for the transfer of delivered RF-energy by the antennas. SMS7630 series pair Schottky diode [81] has been selected. Fig. 10 depicts the proposed diode model's equivalent circuit. The rectifier circuit is designed by using ADS simulation with a dimension is [18×20×1.6] mm^3 and operates at (2.3-6) GHz. It is insensitive to a broad range of RF-input power levels between (-15dBm to 5dBm). At a 0dBm input-power, the max simulated and measured PCE of 67.8% and 65.1% respectively, with output voltages of 1.68V and 1.65V.

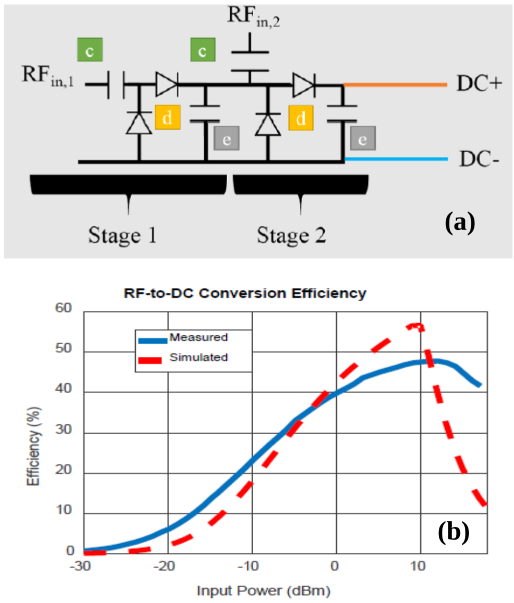

Fig. 9. Proposed RF-DC rectifier circuit design [88]: (a) Circuit diagram, (b) Power conversion efficiency PCE versus input power.

Fig. 10. Schematic View of the rectifying diode equivalent circuit (Top) and numerical results (bottom) [89].

There are several challenges for the design of the rectifying circuit since the input-power is very low less than -20dBm. However, there are published studies that focus on embedded rectifiers [90].

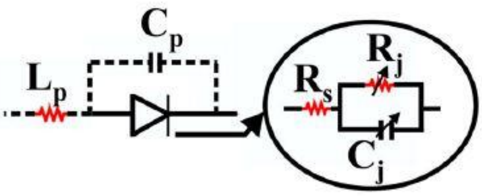

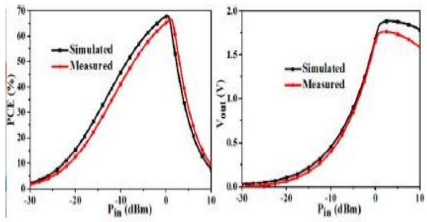

Ding, et al. presented a new rectifying circuit topology for medical applications in 2020 [91]. This model is built with off-the-shelf components and tested at MICS bands. This work employs a single diode and VDR circuit constructed by using HSMS-2850 and Skyworks 7630 diodes, as illustrated in Fig. 11. (a). To achieve a small size design of implant rectenna, the surfaces of the implanted antenna and rectifier are fit, which means the same size during PCB production, as illustrated in Fig. 11. (b). According to the results in Fig. 12, when the source produces a total power of -20dBm, the rectifying efficiency is 31.15%, and the output voltage is 0.195V. Compared with the rectifier efficiency is 41.2% at -16dBm of input power and which is 10% better.

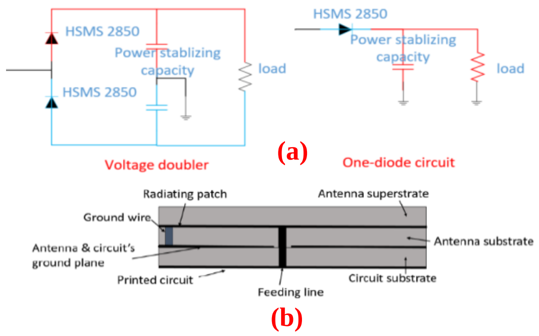

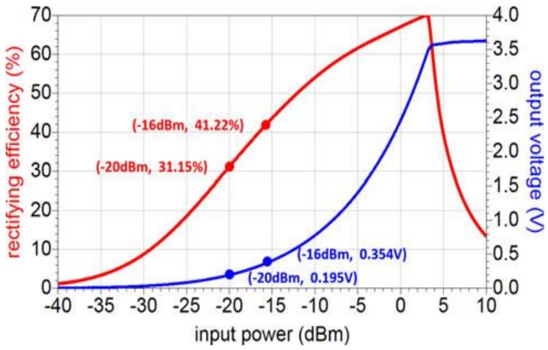

Fig. 11. Rectenna system structure [91]: (a)

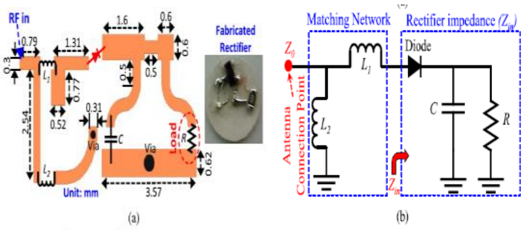

Rectifying circuit design using HSMS-2850 diode. (b) the Physical structure of the rectenna system.

Fig. 12. The measured output voltages and Efficiencies at different source power [91].

In 2021 [92], Iqbal, et al. suggested a new implant WPT design called the implant rectifying antenna. The proposed rectenna uses dual bands of 915MHz and 1470MHz to generate sufficient dc energy for charging and driving deep-tissue IMDs. At a resonance frequency of 1470MHz, the authors proposed a compact rectifier circuit with size of [3.4 × 6.7] mm^2. As shown in Fig. 13 and table 7, the suggested circuit has a high conversion efficiency of 50% even at an input power of -14 dBm and a maximum efficiency of 76.1% at 2 dBm.

Fig. 13. Compact design of the implant rectifier circuit [92]: (a) schematic and fabricated prototype, and (b) equivalent circuit of the rectifier. L_1=22nH, L_2 =4nH, R=2kΩ, and C=12pF.

Table 7. Performance comparison of different structures implant rectifier-design

Ref.	Freq. [GHz]	Rectifier Topology	Pin [dBm]	PCE [%]	Vout [V]	Load [KΩ]
[88] 2018	2.4	Voltage Quadruple	0	40	1	1.8
[89] 2021	2.45	Voltage Doubler Rectifier	0	65.1	1.65	4.1
[90] 2019	0.403	CMOS process	2	15.5	---	---
[91] 2020	0.403 0.915	VDR	-20	31.15	0.195	13
[92] 2021	0.935 0.147	One diode topology	2	76.1	1.48	2 10.9
[93] 2019	2.4	Series, Shunt, VDR	-20	25	---	4.3
	2.45		-10	40		
[94] 2020	0.147	VDR	2	90	4	---
[95] 2020	2.45	VD	25	80.2	---	0.4
[96] 2021	5.8	N-stage HTVM	32	67	19.8	1.5

[97] 2019	5.8	Dickson charge pump	21-25	64	34.2	1
[98] 2020	0.17	Bridge diode	27	86	3	---
	2.4			75		
[99] 2021	0.184	VDR	-4	79.46	1.5	5
	0.242			86.32		

4. MINIATURIZED IC RECTENNA CIRCUITS DESIGN

In the previous two sections, the design and performance analysis of different implantable antenna structures followed by fabrication and characterization has been discussed in tables 3, 4, and 5. Another substantial component of the rectenna's system is the rectifier. The rectifier assists in the conversion of RF signals received into electrical DC. Table 7 shows the rectifier configurations that have been reported thus today.

In this section, we discuss the advanced miniaturized rectenna IC for IMDs devices. This section describes how to design a rectenna to achieve the required characteristics such as high gain, compact size, and high PCE through suggest a new structure of the rectenna design such as folded dipole antenna with a half-wave low- power rectifier circuit [100]. The implant rectenna system consists of an embedded antenna and implant rectifying circuits as discussed in sections 2, and 3 respectively. In this article, different compact rectennas designs have been investigated as shown in table 8, and the most recently reported is presented based on miniaturization techniques used for size reduction of the rectenna. Bhatt, et al. presented a sickle-shaped fractal structure for compact rectenna that operate at dual bands [101]. At an optimum load resistor of 600Ω, the proposed rectenna has a measured efficiency of 63% and 54.8% at 2.4GHz and 5.8GHz, respectively.

Minh, et al. in 2021 [102], proposed a new meandered structure of the compact rectenna used for RF energy harvesting such as 3G and 4G technology as shown in Fig. 14. The rectenna is operated at 2.14GHz with a maximum PCE of 62% at optimum load resistor is 1.2kΩ. A circularly polarized meandered-loop antenna has been used to achieve a compact size of rectenna is [30 x 50 x 0.8] mm^3 and measured bandwidth of 150MHz at 0dBm of input power.

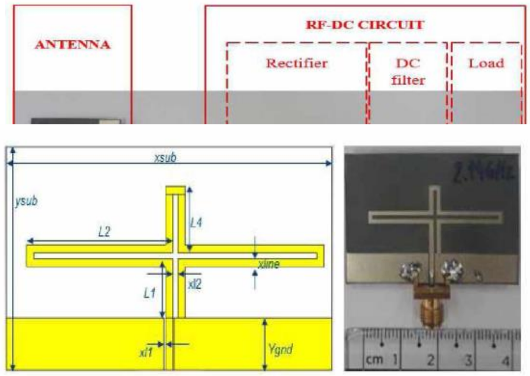

Fig. 14. The proposed CP-meandered loop antenna structure and prototype [102]. Dimensions in mm. x_{sub}=45mm, L_1=7mm, y_{sub}=30, L_2=17.6mm, Y_{gnd}=7, x_{line}=1.1, xl_1=0.3, and xl_2=0.8

Assogba, et al. in 2021 [103], presented a new fractal geometry structure of the rectenna design for energy-harvesting is shown in Fig. 15. They suggest a rectangular patch antenna with a small size printed on the FR-4 substrate to convert RF-DC rectifying. The proposed rectenna has a frequency of 2.45GHz. This design was simulated using HFSS and ADS software. At 0dBm input power, the efficiency is 54%, the bandwidth is 150MHz with a return loss of 52dB, and a peak gain of 3.48dB.

Fig. 15. The proposed fractal geometry structure of the rectenna [103]: Ws=40, Ls=47.5, Lg=30.5,

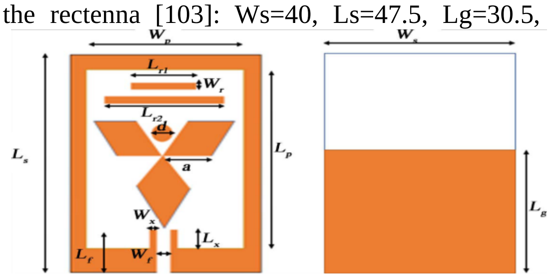

Lx=5, Wp=32, Wx=1.75, Lp=42, Lr1=15, Wf=3, Lr2=25, Lf=7, Wr=3, a=10, d=4.

Many RF-bands have recently been made available for different uses, and the availability of ambient radio frequency power levels is increased as more radio transmitters are developed. As a result, rectenna-based applications of the wireless energy harvesting WEH technique are becoming more prominent. The performance of rectenna systems for the different bands used in WEH applications is presented in table 9. Such as single-band in [106], [107], [108], dual-band [109], [110], [111], multi-band [112], and broadband rectennas [113], [114].

Wireless body area networks and their applications in the field of telemedicine have received a lot of attention in recent years.

Implantable medical devices, in general, are widely utilized to transmit critical data. Its development opens up opportunities for patients, especially those with chronic diseases, to have a better quality of life. The issue of power supply also arises as a result of the implanted equipment' long-term use. Wireless power transfer (WPT) could reduce the need for many surgeries and health problems. As a result, WPT applications have been achieved using implantable rectennas. As shown in table 10, we will describe many configurations of the rectenna design that operate in medical bands such MICS and ISM.

Table 8. Comparison of compact rectenna design with different techniques for size reduction.

Ref. Year	Rectenna Configuration	Freq. Band [GHz]	Size reduction technique	Size of rectenna [mm^3]	Rectifier circuit topology	Maximum efficiency [%]	Pin [dBm] / R_L [kΩ]
[28] 2021	Multiband triple L-Arms patch antenna with slot ground	10	Slotted	19.7 ×7.4 ×0.81	VDR	43	6 / 0.65
[30] 2021	Wideband circular polarized slot microstrip rectenna	1.85		---	---	69	12 / 1
		2.45				64	10 / 1
[34] 2022	C-shaped circularly polarized implant rectenna	2.4		7.5 × 7.5 × 1.27	VDR HSMS 2852	45	0 / 2
[89] 2021	Compact circularly polarized CP hexagonal-shaped	2.45		2 × 2 × 0.04	VDR SMS-7630	65.1	0 / 4.1
[58] 2019	Meander integrated E-shaped	2.15	Meandered antenna	60 × 60 × 4.6	VDR SMS7630	55	3 / 1.8
[101] 2019	Sickle-shaped antenna with IMN	2.4		80 × 48 × 1.6	Half-wave HSMS-2860	67.62	25 / 0.6
		5.8				59.62	
[102] 2021	Circularly polarized meandered-loop	2.14		30 × 50 × 0.8	SMS-7630	62	0 / 1.2
[104] 2020	Fractal monopole antenna array	0.91-2.55	Fractal	165 × 165 × 0.8	Full-wave HSMS-285C	68	-10 / 4.7
[103] 2021	Patch Rectangular	2.45		40 × 47.5 × 1.6	Series diode HSMS-2850	54	0 / 1
[78] 2021	Compact octagonal broadband rectenna with DGS	1.975–4.744	Defected Ground Structure	40 × 45 × 1.6	VDR HSMS-270B	88.58	0 / 100
[105] 2021	Compact Coplanar waveguide with irregular slotted symmetrical M-shape microstrip	5.8	Coplanar waveguide feed	25 × 30 × 1.6	VDR	---	---

Table 9. Performance of different band rectenna system for energy harvesting.

Ref. Year	Bands	Operating Frequency [GHz]	ε_r	Rectifier Topology	Antenna Bandwidth [GHz]	Peak Gain [dBi]	PCE [%]	Pin [dBm]
[106] 2020	Single Band Application	5.8	2.2	HWR	5.77-5.84	14.2	82.4	11
[107] 2019		5.8	2.1	VDR	5.5-6.7	8.56	73.4	-6
[108] 2019		0.9	3.38	VDR	0.88 - 0.92	2.17	81	-7.6
[109]		2.4	4.4		2.39-2.52	5.5	45	10

2018		5.8		4-stage VDR HSMS2850	5.65-5.85	6.3		
[110] 2020	Dual Band Application	3.5	2.2	Dual-band Rectifier SMS-7630	0.21	10.2	45	0
		5.8			0.4	8.92	29	
[111] 2021		0.9	5.4	Dual-band Rectifier HSMS2850	0.15	0.62	12.93	-30
		1.8			0.2	2.36	8	
[112] 2020	Multi-band Application	1.8	4.3	Modified hybrid ring SMS-7630	0.032	2.41	68	10
		2.1			0.096	2.26	26	
		2.45			0.098	1.58	42	
		2.6			0.138	2.69	64	
[113] 2019	Broad band application	1.5-2.7	--	VDR	1.7-2.6	2.9	50	5
[114] 2020		22.5-27.5	4.4	VDR	22.5-27.5	7.8	80	5

Table 10. Performance of different structures implantable rectenna for medical applications.

Ref. Year	Miniaturization Techniques	Freq. Bands [GHz]	Dimensions in [mm]	Rectifier Topology	Medical Applications
[34] 2022	CP implantable antenna with four C-shaped open slots	2.4–2.48	7.5 x 7.5 x 1.27	VDR Rectifier	Microwave WPT
[88] 2018	Near-field radiating patch antennas	2.4	27.5 x 19.75 x 2.06	Voltage Quadrupler rectifier	Wirelessly power sensor devices from near-field radiation patch antennas
[90] 2018	Wearable RF-powered rectenaa leadless pacing system	0.924	164 x 86 x 0.25	Voltage multiplier	The management of heart failure patients via the implantation of cardiac pacemakers.
[91] 2020	Miniaturized circular implant integrated rectenna	0.403	π x $(5.4)^2$ x 0.64	VDR HSMS-2850	Biomedical wireless applications such as (IMD).
		0.915			
[115] 2019	Arm-implantable rectenna by dual band PIFA with slit/slot loading.	Med-Radio 0.401 - 0.406	16 x 14 x 1.27	One-series diode and Voltage doubler	Wireless power transfer at ISM band, and wireless data telemetry at MedRadio
		ISM 0.9028 - 0.928			
[116] 2019	Wireless RF to DC implantable power rectifying system	ISM 0.9028 - 0.928	π x $(5.4)^2$ x 0.64	VDR SMS 7630	Biomedical WPTs for implantable medical device (IMD).
[117] 2019	Near-field Implant Rectenna system by using self-phasing.	0.915	50 × 40 × 1.6	Implantable single diode HSMS2852	Near-field biomedical applications
[118] 2021	Bipolar spiral Tx structure, and hooked-shaped.	1.87	12.5 x 12 x 0.5	---	Cardiac Implants Application

5. CONCLUSION

After reviewing around 120 published articles on rectenna systems, Rectenna is a versatile microwave circuit with various applications, including WPT, WSN, implantable medical devices IMDs, and energy harvesting.

The design of the rectenna system for various applications has been highlighted in this review study. The operating frequency of the rectenna system design must be chosen based on the availability of ambient energy in the surrounding environment. Many frequency bands are used in the RF energy harvesting applications such as Mobile, WLAN, and Medical bands.

Tables 3–10 show a variety of miniaturization techniques for implant rectenna design that has been described in this review. The planar folded antenna with fractal is the most common structure for IMDs. Therefore, by using this structure, we can obtain a compact rectenna design with a small size and the best properties such as conversion efficiency, peak gain, radiation pattern, SAR value, and optimum load at a certain input power.

The rectifying circuits design is the most important part of the rectenna system design for energy harvesting due to enhance DC output voltage and PCE. For all researchers, designing a rectifier with a higher conversion efficiency is a difficult task due to its mismatches with the antenna. The topology of the chosen diode has a significant impact on the rectifier circuit's performance. The optimal PCE and output voltage are provided by the VDR configuration.

In my opinion, this review paper will be helpful to researchers in choosing a suitable configuration to meet the specific requirements for their desired applications. Specifically, I chose the current references which operated at the miniaturization implantable IC Rectenna for implantable medical devices IMDs are mentioned in the tables from 3 to 10.

REFERENCES

[1] M. Kumar, "Social, economic, and environmental impacts of renewable energy resources," *Wind Solar Hybrid Renewable Energy System*, vol. 1, 2020.

[2] H. Liu, H. Fu, L. Sun, C. Lee, and E. M. Yeatman, "Hybrid energy harvesting technology: From materials, structural design, system integration to applications," *Renewable and sustainable energy reviews*, vol. 137, p. 110473, 2021.

[3] P. Jiao, W. Borchani, H. Hasni, and N. Lajnef, "Enhancement of quasi-static strain energy harvesters using non-uniform cross-section post-buckled beams," *Smart Materials and Structures*, vol. 26, no. 8, p. 085045, 2017.

[4] A. Mohammadnia, A. Rezania, B. M. Ziapour, F. Sedaghati, and L. Rosendahl, "Hybrid energy harvesting system to maximize power generation from solar energy," *Energy Conversion and Management*, vol. 205, p. 112352, 2020.

[5] Q. Wen, X. He, Z. Lu, R. Streiter, and T. Otto, "A comprehensive review of miniatured wind energy harvesters," *Nano Materials Science*, vol. 3, no. 2, pp. 170–185, 2021.

[6] A. Nozariasbmarz et al., "Review of wearable thermoelectric energy harvesting: From body temperature to electronic systems," *Applied Energy*, vol. 258, p. 114069, 2020.

[7] R. Subbaramaiah, S. A. Al-Jufout, A. Ahmed, and M. M. Mozumdar, "Design of vibration-sourced piezoelectric harvester for battery-powered smart road sensor systems," *IEEE Sensors Journal*, vol. 20, no. 23, pp. 13940–13949, 2020.

[8] S. Roy, J.-J. Tiang, M. B. Roslee, M. Ahmed, A. Z. Kouzani, and M. Mahmud, "Design of a Highly Efficient Wideband Multi-Frequency Ambient RF Energy Harvester," *Sensors*, vol. 22, no. 2, p. 424, 2022.

[9] S. A. A. Shah and H. Yoo, "Radiative near-field wireless power transfer to scalp-implantable biotelemetric device," *IEEE Transactions on Microwave Theory and Techniques*, vol. 68, no. 7, pp. 2944–2953, 2020.

[10] M. T. Bevacqua, G. G. Bellizzi, and M. Merenda, "An efficient far-field wireless power transfer via field intensity shaping techniques," *Electronics*, vol. 10, no. 14, p. 1609, 2021.

[11] A. M. Sabaawi and O. A. Al-Ani, "Solar Rectennas: Analysis and Design," in *Recent Wireless Power Transfer Technologies, IntechOpen*, 2019.

[12] M. Al-Hasan, P. R. Sura, A. Iqbal, J. J. Tiang, I. B. Mabrouk, and M. Nedil, "Low-profile dual-band implantable antenna for compact implantable biomedical devices," *AEU-International Journal of Electronics and Communications*, vol. 138, p. 153896, 2021.

[13] N. Marriwala, "Energy Harvesting System Design and Optimization Using High Bandwidth Rectenna for Wireless Sensor Networks," *Wireless Personal Communications*, vol. 122, no. 1, pp. 669–684, 2022.

[14] P. Sharma and A. K. Singh, "A Compact Antenna Design With High Gain for Wireless Energy Harvesting," in *Computational Methodologies for Electrical and Electronics Engineers, IGI Global*, 2021, pp. 244–253.

[15] N. Saranya and T. Kesavamurthy, "Review on next generation wireless power transmission technology for implantable biomedical devices," *International Journal of Biomedical Engineering and Technology*, vol. 35, no. 3, pp. 207–222, 2021.

[16] A. N. Khan, Y. Cha, H. Giddens, and Y. Hao, "Recent advances in organ specific wireless bioelectronic devices: Perspective on biotelemetry and power transfer using antenna systems," *Engineering*, 2022.

[17] M. N. Hasan, S. Sahlan, K. Osman, and M. S. Mohamed Ali, “Energy harvesters for wearable electronics and biomedical devices,” *Advanced Materials Technologies*, vol. 6, no. 3, p. 2000771, 2021.

[18] V. Sadadiwala, K. Mahindroo, V. Singh, P. Bansal, and S. Singhal, “Human Body Monitoring Wearable Antenna,” in *Optical and Wireless Technologies*, Springer, 2022, pp. 151–161.

[19] M. Zellagui, *Wireless Power Transfer: Recent Development, Applications and New Perspectives*. BoD–Books on Demand, 2021.

[20] M. Song et al., “Wireless power transfer based on novel physical concepts,” *Nature Electronics*, vol. 4, no. 10, pp. 707–716, 2021.

[21] L. J. Zou, Y. Liu, Y.-G. Su, and A. P. Hu, “Study of power flow mechanism of capacitive power transfer system based on Poynting vector analysis,” *International Journal of Electrical Power & Energy Systems*, vol. 134, p. 107374, 2022.

[22] J. Bao, S. Hu, Z. Xie, G. Hu, Y. Lu, and L. Zheng, “Optimization of the Coupling Coefficient of the Inductive Link for Wireless Power Transfer to Biomedical Implants,” *International Journal of Antennas and Propagation*, vol. 2022, 2022.

[23] H. K. Behera and D. P. Kar, “Preliminary Study of Magnetic Resonant Coupling Based Wireless Power Transfer System,” in *Green Technology for Smart City and Society,* Springer, 2021, pp. 377–384.

[24] S. R. Khan, S. K. Pavuluri, G. Cummins, and M. P. Desmulliez, “Wireless power transfer techniques for implantable medical devices: A review,” *Sensors,* vol. 20, no. 12, p. 3487, 2020.

[25] J. Kim et al., “Active photonic wireless power transfer into live tissues,” *Proceedings of the National Academy of Sciences*, vol. 117, no. 29, pp. 16856–16863, 2020.

[26] Z. Kashani, S. J. J. Ilham, and M. Kiani, “Design and Optimization of Ultrasonic Links with Phased Arrays for Wireless Power Transmission to Biomedical Implants,” *IEEE Transactions on Biomedical Circuits and Systems*, 2022.

[27] A. D. Boursianis et al., “Triple-band single-layer rectenna for outdoor RF energy harvesting applications,” *Sensors*, vol. 21, no. 10, p. 3460, 2021.

[28] D. H. Sadek, H. A. Shawkey, and A. A. Zekry, “Compact and High-Efficiency Rectenna for Wireless Power-Harvesting Applications,” *International Journal of Antennas and Propagation*, vol. 2021, 2021.

[29] H. Sun, J. Huang, and Y. Wang, “An Omnidirectional Rectenna Array With An Enhanced RF Power Distributing Strategy for RF Energy Harvesting,” *IEEE Transactions on Antennas and Propagation*, 2022.

[30] M. M. Fakharian, “A high gain wideband circularly polarized rectenna with wide ranges of input power and output load,” *International Journal of Electronics*, pp. 1–17, 2021.

[31] E. Kwiatkowski, J. A. Estrada, A. López-Yela, and Z. Popović, “Broadband RF Energy-Harvesting Arrays,” *Proceedings of the IEEE*, vol. 110, no. 1, pp. 74–88, 2022.

[32] H. Yadav, K. P. Ray, and M. Gupta, “Differential microstrip patch rectenna featuring consistent high gain over a wide operating bandwidth,” *Microwave and Optical Technology Letters*, vol. 63, no. 5, pp. 1470–1476, 2021.

[33] P. Chindhi, H. Rajani, and G. Kalkhambkar, “A Tapered Slot Rectangular Ultra-wideband Microstrip Patch Antenna for Radio Frequency Energy Harvesting,” in *Futuristic Communication and Network Technologies*, Springer, 2022, pp. 373–383.

[34] C. Xu, Y. Fan, and X. Liu, “A Circularly Polarized Implantable Rectenna for Microwave Wireless Power Transfer,” *Micromachines*, vol. 13, no. 1, p. 121, 2022.

[35] Q. Awais, A. Farooq, W. Ali, R. Afzal, and A. Khalid, “A Novel Wideband Coplanar Waveguide (CPW) Fed Antenna for Energy Harvesting at 2.45 GHz,” *Engineering Proceedings*, vol. 12, no. 1, p. 54, 2022.

[36] P. K. Mishu and I. Song, “Highly-Efficient CMOS Rectifier for Wide Range of Input RF Power in Energy-Harvesting Systems,” 2021, pp. 75–79..

[37] Y. Feng, Z. Li, L. Qi, W. Shen, and G. Li, “A compact and miniaturized implantable antenna for ISM band in wireless cardiac pacemaker system,” *Scientific Reports*, vol. 12, no. 1, pp. 1–11, 2022.

[38] M. J. Karimi, A. Schmid, and C. Dehollain, “Wireless power and data transmission for implanted devices via inductive links: a systematic review,” *IEEE Sensors Journal*, vol. 21, no. 6, pp. 7145–7161, 2021.

[39] N. A. Malik, P. Sant, T. Ajmal, and M. Ur-Rehman, “Implantable antennas for bio-medical applications,” *IEEE Journal of Electromagnetics, RF and Microwaves in Medicine and Biology*, vol. 5, no. 1, pp. 84–96, 2020.

[40] M. Abdul-Al et al., “Wireless Electromagnetic Radiation Assessment Based on the Specific Absorption Rate (SAR): A Review Case Study,” *Electronics*, vol. 11, no. 4, p. 511, 2022.

[41] M. Zhuk and J. Paradis, “An Efficient Approximation of Frequency and Temperature-Dependent Dielectric Properties of Tissues.,” *Progress in Electromagnetics Research B*, vol. 91, 2021.

[42] S. Di Meo et al., “The variability of dielectric permittivity of biological tissues with water content,” *Journal of Electromagnetic Waves and Applications*, vol. 36, no. 1, pp. 48–68, 2022.

[43] G. Shin and I.-J. Yoon, “Investigation on insulated, brain-implanted antenna for highly reliable biotelemetry communication in MICS and ISM bands,” *Sensors*, vol. 20, no. 1, p. 242, 2019.

[44] A. Alemaryeen and S. Noghanian, “On the Effects of Balun on Small Antennas Performance for Animal Health-Monitoring and Tracking,” *Advanced Electromagnetics*, vol. 10, no. 2, pp. 39–43, 2021.

[45] N. H. Abd Rahman, Y. Yamada, and M. S. Amin Nordin, “Analysis on the effects of the human body on the performance of electro-textile antennas for

wearable monitoring and tracking application," *Materials*, vol. 12, no. 10, p. 1636, 2019.

[46] J. Zhang, R. Das, J. Zhao, N. Mirzai, J. Mercer, and H. Heidari, "Battery-Free and Wireless Technologies for Cardiovascular Implantable Medical Devices," *Advanced Materials Technologies*, p. 2101086, 2021.

[47] P. G. Paga, H. Nagaraj, R. Tejas, and V. Sanath, "Design and Analysis of Dual-Band Monopole Antenna Using Star EBG Structures," in *Emerging Research in Computing, Information, Communication and Applications*, Springer, 2022, pp. 755–767.

[48] M. Samad, M. M. Rahman, and S. Shamim, "Design of a Miniaturized Implantable PIFA with DGS for the Investigation of Uterus Fibroids," 2021.

[49] R. B. Khadase, A. Nandgaonkar, B. Iyer, and A. Wagh, "Multilayered Implantable Antenna Biosensor for Continuous Glucose Monitoring: Design and Analysis," *Progress In Electromagnetics Research C*, vol. 114, pp. 173–185, 2021.

[50] S. Sukhija, R. K. Sarin, and N. Kashyap, "Design of compact wideband serpentine patch antenna for ingestible endoscopic applications," *Progress In Electromagnetics Research M*, vol. 66, pp. 53–63, 2018.

[51] A. Rula, "Patch antenna based on spiral split rings for bone implants," Przegląd Elektrotechniczny, vol. 96, 2020.

[52] T.-A. Le Trong, S. I. H. Shah, G. Shin, S. M. Radha, and I.-J. Yoon, "A compact triple-band antenna with a broadside radiation characteristic for head-implantable wireless communications," *IEEE Antennas and Wireless Propagation Letters*, vol. 20, no. 6, pp. 958–962, 2021.

[53] N. Samsuri, M. Rahim, F. Seman, and M. Inam, "Compact meander line telemetry antenna for implantable pacemaker applications," *Indones. J. Electr. Eng. Comput. Sci*, vol. 10, pp. 883–889, 2018.

[54] N. Pournoori, L. Sydänheimo, Y. Rahmat-Samii, L. Ukkonen, and T. Björninen, "Small Triple-Band Meandered PIFA for Brain-Implantable Biotelemetric Systems: Development and Testing in a Liquid Phantom," *International Journal of Antennas and Propagation*, vol. 2021, 2021.

[55] Y. Fan, H. Liu, X. Liu, Y. Cao, Z. Li, and M. M. Tentzeris, "Novel coated differentially fed dual-band fractal antenna for implantable medical devices," *IET Microwaves, Antennas & Propagation*, vol. 14, no. 2, pp. 199–208, 2020.

[56] F. Faisal and H. Yoo, "A miniaturized novel-shape dual-band antenna for implantable applications," *IEEE Transactions on Antennas and Propagation*, vol. 67, no. 2, pp. 774–783, 2018.

[57] C. Gayathri and S. Venkatanarayanan, "A miniaturized circular maze shaped antenna for implantable health care applications," *Journal of Ambient Intelligence and Humanized Computing*, vol. 12, no. 5, pp. 4757–4763, 2021.

[58] K. Çelik and E. Kurt, "A novel meander line integrated E-shaped rectenna for energy harvesting applications," *International Journal of RF and Microwave Computer-Aided Engineering*, vol. 29, no. 1, p. e21627, 2019.

[59] D. Surender, T. Khan, and F. A. Talukdar, "A hexagonal-shaped microstrip patch antenna with notch included partial ground plane for 2.45 GHz Wi-Fi band RF energy harvesting applications," 2020, pp. 966–969.

[60] D. Surender, T. Khan, and F. A. Talukdar, "A pentagon-shaped microstrip patch antenna with slotted ground plane for RF energy harvesting," 2020, pp. 1–4.

[61] A. Meftahi et al., "Nanocelluloses as skin biocompatible materials for skincare, cosmetics, and healthcare: Formulations, regulations, and emerging applications," *Carbohydrate Polymers*, vol. 278, p. 118956, 2022.

[62] T. Sathiyapriya, V. Gurunathan, and J. Dhanasekar, "Design of an implantable antenna for biomedical applications," 2021.

[63] G. Rathee, G. Bartwal, J. Rathee, Y. K. Mishra, A. Kaushik, and P. R. Solanki, "Emerging Multimodel Zirconia Nanosystems for High-Performance Biomedical Applications," *Advanced NanoBiomed Research*, vol. 1, no. 9, p. 2100039, 2021.

[64] K. Yeap, C. Voon, T. Hiraguri, and H. Nisar, "A compact dual-band implantable antenna for medical telemetry," *Microwave and Optical Technology Letters*, vol. 61, no. 9, pp. 2105–2109, 2019.

[65] M. Usluer, B. Cetindere, and S. C. Basaran, "Compact implantable antenna design for MICS and ISM band biotelemetry applications," *Microwave and Optical Technology Letters*, vol. 62, no. 4, pp. 1581–1587, 2020.

[66] M. Wang et al., "Broadband implantable antenna for wireless power transfer in cardiac pacemaker applications," *IEEE Journal of Electromagnetics, RF and Microwaves in Medicine and Biology*, vol. 5, no. 1, pp. 2–8, 2020.

[67] M. Seydi and M. S. Bayati, "Design, Simulation and Fabrication of an Implanted Antenna at ISM Band in Body Tissue," *Wireless Personal Communications*, vol. 122, no. 3, pp. 2023–2033, 2022.

[68] R. Kumar, S. Singh, and A. P. S. Chauhan, "Implantable Antenna Design Based on Gosper Curve Fractal Geometry," *IETE Journal of Research*, pp. 1–11, 2021.

[69] R. Kumar, L. S. Solanki, and S. Singh, "Miniature Archimedean spiral PIFA antennas for biomedical implantable devices," in *2019 6th International Conference on Signal Processing and Integrated Networks (SPIN)*, 2019, pp. 162–167.

[70] N. Ganeshwaran, J. K. Jeyaprakash, M. G. N. Alsath, and V. Sathyanarayanan, "Design of a dual-band circular implantable antenna for biomedical applications," *IEEE Antennas and Wireless Propagation Letters*, vol. 19, no. 1, pp. 119–123, 2019.

[71] M. M. Khan and T. Hossain, "Compact Planar Inverted F Antenna (PIFA) for Smart Wireless Body Sensors Networks," vol. 2, no. 1, p. 63, 2020.

[72] Z.-J. Yang and S. Xiao, "A wideband implantable antenna for 2.4 GHz ISM band biomedical application," in *2018 International Workshop on Antenna Technology (iWAT)*, 2018, pp. 1–3.

[73] A. Garhwal *et al.*, "Wideband circular shaped fractal patch antenna for 2.45 GHz biomedical applications," in *2019 IEEE Asia-Pacific Conference on Applied Electromagnetics (APACE)*, 2019, pp. 1–5.

[74] S. Muhammad, J. Jiat Tiang, S. Kin Wong, A. Iqbal, M. Alibakhshikenari, and E. Limiti, "Compact rectifier circuit design for harvesting GSM/900 ambient energy," *Electronics*, vol. 9, no. 10, p. 1614, 2020.

[75] Hussein, Shamil H. "Design and Simulation of a High Performance CMOS Voltage Doublers using Charge Reuse Technique, " *Journal of Engineering Science and Technology 12.12*, pp. 3344-3357, 2017

[76] D. Surender, T. Khan, F. A. Talukdar, A. De, Y. M. Antar, and A. P. Freundorfer, "Key components of rectenna system: A comprehensive survey," *IETE Journal of Research*, pp. 1–27, 2020.

[77] Hussein, Shamil H., and Mohammad Tariq Yaseen, "Performance Evaluation of Low-Voltage CMOS Switched-Capacitor Circuit, " in *2021 8th International Conference on Electrical and Electronics Engineering (ICEEE)*, IEEE, 2021.

[78] R. Pandey, A. K. Shankhwar, and A. Singh, "An improved conversion efficiency of 1.975 to 4.744 GHz rectenna for wireless sensor applications," *Progress In Electromagnetics Research C*, vol. 109, pp. 217–225, 2021.

[79] S. Tian, X. Zhang, X. Wang, J. Han, and L. Li, "Recent advances in metamaterials for simultaneous wireless information and power transmission," *Nanophotonics*, 2022.

[80] S. El Mattar, A. Baghdad, and A. Ballouk, "A Novel Two-Branch Dual-Band Rectifier for 2.45 GHz 5.8 GHz RFID Systems," in *WITS 2020*, Springer, 2022, pp. 943–948.

[81] L. Zhu, J. Zhang, W. Han, L. Xu, and X. Bai, "A novel RF energy harvesting cube based on air dielectric antenna arrays," *International Journal of RF and Microwave Computer-Aided Engineering*, vol. 29, no. 1, p. e21636, 2019.

[82] J. Liu, M. Huang, Y. Lu, and R. P. Martins, "RF Rectifiers With Wide Incident Angle of Incoming Waves Based on Rat-Race Couplers," *IEEE Transactions on Microwave Theory and Techniques*, 2021.

[83] I. S. A. Razak and Z. Hamid, "Optimization of Rectifying Circuit for RF Energy Scavenging," *ANP Journal of Social Science and Humanities*, vol. 2, no. 1, pp. 60–67, 2021.

[84] S. Salleh, M. A. Zakariya, and R. M. A. Lee, "A Comparison Study of Rectifier Designs for 2.45 GHz EM Energy Harvesting," *Energy and Power Engineering*, vol. 13, no. 2, pp. 81–89, 2021.

[85] Z. Zhou and Y. Chang, "A Novel 5.8 GHz Harmonic-suppressed Rectenna for Wireless Power Transmission," in *2021 International Applied Computational Electromagnetics Society (ACES-China) Symposium*, 2021, pp. 1–2.

[86] N. Hassan et al., "Design of dual-band microstrip patch antenna with right-angle triangular aperture slot for energy transfer application," *International Journal of RF and Microwave Computer-Aided Engineering*, vol. 29, no. 1, p. e21666, 2019.

[87] T. Oh, T. Lim, and Y. Lee, "A Self-Matching Rectifier Based on an Artificial Transmission Line for Enhanced Dynamic Range," *IEEE Transactions on Circuits and Systems I: Regular Papers*, 2022.

[88] B. J. DeLong, A. Kiourti, and J. L. Volakis, "A radiating near-field patch rectenna for wireless power transfer to medical implants at 2.4 GHz," *IEEE Journal of Electromagnetics, RF and Microwaves in Medicine and Biology*, vol. 2, no. 1, pp. 64–69, 2018.

[89] D. Surender, M. A. Halimi, T. Khan, F. A. Talukdar, S. K. Koul, and Y. M. Antar, "2.45 GHz Wi-Fi band operated circularly polarized rectenna for RF energy harvesting in smart city applications," *Journal of Electromagnetic Waves and Applications*, vol. 36, no. 3, pp. 407–423, 2022.

[90] S. M. Asif, A. Iftikhar, J. W. Hansen, M. S. Khan, D. L. Ewert, and B. D. Braaten, "A novel RF-powered wireless pacing via a rectenna-based pacemaker and a wearable transmit-antenna array," *IEEE Access*, vol. 7, pp. 1139–1148, 2018.

[91] S. Ding, S. Koulouridis, and L. Pichon, "Miniaturized implantable power transmission system for biomedical wireless applications," *Wireless Power Transfer*, vol. 7, no. 1, pp. 1–9, 2020.

[92] A. Iqbal, M. Al-Hasan, I. B. Mabrouk, A. Basir, M. Nedil, and H. Yoo, "Biotelemetry and wireless powering of biomedical implants using a rectifier integrated self-diplexing implantable antenna," *IEEE Transactions on Microwave Theory and Techniques*, vol. 69, no. 7, pp. 3438–3451, 2021.

[93] H. P. Paz, V. S. Silva, E. V. Cambero, H. X. Araújo, I. R. Casella, and C. E. Capovilla, "A survey on low power RF rectifiers efficiency for low cost energy harvesting applications," *AEU-International Journal of Electronics and Communications*, vol. 112, p. 152963, 2019.

[94] A. Basir and H. Yoo, "Efficient wireless power transfer system with a miniaturized quad-band implantable antenna for deep-body multitasking implants," *IEEE Transactions on Microwave Theory and Techniques*, vol. 68, no. 5, pp. 1943–1953, 2020.

[95] Z. He, H. Lin, H. Zhu, and C. Liu, "A compact high-efficiency rectifier with a simple harmonic suppression structure," *IEEE Microwave and Wireless Components Letters*, vol. 30, no. 12, pp. 1177–1180, 2020.

[96] J. Kim, I. Park, and H. Ku, "Design of a Highly Efficient N-Stage Harmonic Terminated Voltage Multiplier for Wireless Power Transfer," *Energies*, vol. 14, no. 21, p. 7203, 2021.

[97] J. Bae et al., "5.8 GHz high-efficiency RF–DC converter based on common-ground multiple-stack structure," *Sensors*, vol. 19, no. 15, p. 3257, 2019.

[98] S. A. Rotenberg, S. K. Podilchak, P. D. H. Re, C. Mateo-Segura, G. Goussetis, and J. Lee, "Efficient rectifier for wireless power transmission systems,"

IEEE Transactions on Microwave Theory and Techniques, vol. 68, no. 5, pp. 1921–1932, 2020.

[99] A. Trikolikar and S. Lahudkar, “Design & simulation of dual-band rectifier for ambient RF energy harvesting,” *International Journal of Advanced Technology and Engineering Exploration*, vol. 8, no. 83, p. 1383, 2021.

[100] M. U. Hoque, D. Kumar, Y. Audet, and Y. Savaria, “Design and Analysis of a 35 GHz Rectenna System for Wireless Power Transfer to an Unmanned Air Vehicle,” *Energies*, vol. 15, no. 1, p. 320, 2022.

[101] K. Bhatt, S. Kumar, P. Kumar, and C. C. Tripathi, “Highly efficient 2.4 and 5.8 GHz dual-band rectenna for energy harvesting applications,” *IEEE Antennas and Wireless Propagation Letters*, vol. 18, no. 12, pp. 2637–2641, 2019.

[102] M. T. Le, H. S. Vu, T. Truong, H. T. Vu, and Q. C. Nguyen, “Circularly polarized meandered-loop antenna for ambient RF energy harvesting system,” in *2020 IEEE Eighth International Conference on Communications and Electronics (ICCE)*, 2021, pp. 225–229.

[103] O. Assogba, A. K. Mbodji, S. Diagne, and A. K. Diallo, “Design of a Rectenna in 2.45 GHz Band Frequency for Energy Harvesting,” *Energy and Power Engineering*, vol. 13, no. 9, pp. 333–342, 2021.

[104] M. M. Fakharian, “A wideband rectenna using high gain fractal planar monopole antenna array for rf energy scavenging,” *International Journal of Antennas and Propagation*, vol. 2020, 2020.

[105] P. Sharma and A. K. Singh, “Compact ambient RF energy harvesting CPW Fed Antenna for WLAN,” in *2021 5th international conference on trends in electronics and informatics (ICOEI)*, 2021, pp. 596–600.

[106] D. Kumar and K. Chaudhary, “Design of an improved differentially fed antenna array for RF energy harvesting,” *IETE Journal of Research*, vol. 66, no. 3, pp. 353–358, 2020.

[107] N. Saranya and T. Kesavamurthy, “Design and performance analysis of broadband rectenna for an efficient RF energy harvesting application,” *International Journal of RF and Microwave Computer-Aided Engineering*, vol. 29, no. 1, p. e21628, 2019.

[108] M. Palandoken and C. Gocen, “A modified Hilbert fractal resonator based rectenna design for GSM900 band RF energy harvesting applications,” *International Journal of RF and Microwave Computer-Aided Engineering*, vol. 29, no. 1, p. e21643, 2019.

[109] O. Amjad, S. W. Munir, S. T. Imeci, and A. Ö. Ercan, “Design and implementation of dual band microstrip patch antenna for WLAN energy harvesting system,” *Applied Computational Electromagnetics Society Journal*, 2018.

[110] M. C. Derbal and M. Nedil, “A high gain dual band rectenna for RF energy harvesting applications,” *Progress In Electromagnetics Research Letters*, vol. 90, pp. 29–36, 2020.

[111] S. Muhammad, J. J. Tiang, S. K. Wong, A. Smida, R. Ghayoula, and A. Iqbal, “A dual-band ambient energy harvesting rectenna design for wireless power communications,” *IEEE Access*, vol. 9, pp. 99944–99953, 2021.

[112] A. Benayad and M. Tellache, “A compact energy harvesting multiband rectenna based on metamaterial complementary split ring resonator antenna and modified hybrid junction ring rectifier,” *International Journal of RF and Microwave Computer-Aided Engineering*, vol. 30, no. 2, p. e22031, 2020.

[113] H. Mahfoudi, M. Tellache, and H. Takhedmit, “A wideband rectifier array on dual-polarized differential-feed fractal slotted ground antenna for RF energy harvesting,” *International Journal of RF and Microwave Computer-Aided Engineering*, vol. 29, no. 8, p. e21775, 2019.

[114] N. Singh, S. Kumar, B. K. Kanaujia, M. T. Beg, and S. Kumar, “A compact broadband GFET based rectenna for RF energy harvesting applications,” *Microsystem Technologies*, vol. 26, no. 6, pp. 1881–1888, 2020.

[115] S. Bakogianni and S. Koulouridis, “A dual-band implantable rectenna for wireless data and power support at sub-GHz region,” *IEEE Transactions on Antennas and Propagation*, vol. 67, no. 11, pp. 6800–6810, 2019.

[116] S. Ding, S. Koulouridis, and L. Pichon, “Implantable rectenna system for biomedical wireless applications,” in *2019 IEEE Wireless Power Transfer Conference (WPTC)*, 2019, pp. 454–457.

[117] K. Zhang et al., “Near-field wireless power transfer to deep-tissue implants for biomedical applications,” *IEEE Transactions on Antennas and Propagation*, vol. 68, no. 2, pp. 1098–1106, 2019.

[118] H. Le-Huu and C. Seo, “Bipolar Spiral Midfield Wireless Power Transfer for Cardiac Implants Application,” *IEEE Antennas and Wireless Propagation Letters*, vol. 20, no. 9, pp. 1631–1635, 2021.

مقالة مراجعة للدوائر المتكاملة المتقدمة نوع Rectenna المصغر لتطبيقات حصاد الطاقة

شامل حمزة حسين **خالد خليل محمد**

shamil_alnajjar84@uomosul.edu.iq khalid.khaleel@uomosul.edu.iq

جامعة الموصل - كلية الهندسة - قسم الهندسة الكهربائية - موصل – العراق

تاريخ الاستلام:31-08-2022 استلم بصيغته المنقحة:27-09-2022 تاريخ القبول:0-10-2022

الملخص

تقدم هذه المقالة مراجعة لأنواع مختلفة من تصميم الدوائر المتكاملة للـ Rectenna التي تستخدم بشكل كبير جداً في تطبيقات حصاد الطاقة مثل التطبيقات الطبية. يتكون هذا تصميم من مكونين أساسيين: هوائي مدمج يقوم بجمع طاقة الترددات اللاسلكية من البيئة المحيطة، ودائرة المعدل او المقوم والتي تحول قيم طاقة الترددات الراديوية إلى جهد تيار مستمر من اجل الاستفادة منها واستخدامها في الأجهزة الإلكترونية منخفضة الطاقة ومنها الأجهزة الطبية القابلة للزرع أجهزة (IMDs). تُستخدم ثنائيات الميكروويف نوع الشوتكي مثل HSMS-285x والـ SMS-763x كمقوم مضاعف للجهد مع هوائي مزروع لتحسين كفاءة التحويل والجهد الناتج عند طاقة إدخال معينة وحمل مناسب. هناك العديد من التحديات في تصميم الـــ IC Rectenna القابل للزرع داخل جسم الانسان مثل التوافق الحيوي مع انسجة الجسم، والتصغير، وسلامة المريض، والحجم الصغير، وتردد الرنين، وعرض النطاق الترددي، وكفاءة الإشعاع. تلخص مقالة المراجعة هذه البحث الشامل الذي تم إجراؤه لاستراتيجيات الجديدة في تصميم هياكل مختلفة من دوائر Rectenna المزروعة في التطبيقات الطبية والتي تعمل في النطاقات الصناعية والطبية (ISM Band 2.45GHz, and 5.8GHz).

الكلمات الداله:

الدوائر المتكاملة للــ REctenna، دايود شوتكي، حصاد الطاقة، الهوائيات المزروعة.